*Pharmaceutical Research, Vol. 25, No. 5, May 2008 (© 2007)*
DOI: 10.1007/s11095-007-9507-x

*Research Paper*

# Microdomain pH Gradient and Kinetics Inside Composite Polymeric Membranes of pH and Glucose Sensitivity

**Hui Yu Huang,[1] James Shaw,[2] Christopher Yip,[2] and Xiao Yu Wu[1,3]**

*Received August 4, 2007; accepted November 19, 2007; published online December 11, 2007*

***Purpose.*** Polymeric membranes containing pH-sensitive nano-hydrogels and glucose oxidase were found to exhibit glucose-responsive insulin release. To verify that this glucose-responsiveness stemmed from the decrease in the internal pH of the membranes, we determined the spatial and temporal pH profiles inside the composite membranes *in situ* for the first time.

***Materials and Methods.*** A pH-sensitive fluorescent dye and an inert internal reference was incorporated in the membranes consisting of poly(*N*-isopropylacrylamide-co-methacrylic acid) nanoparticles in a polymer matrix, with or without glucose oxidase and catalase. The fluorescence intensity *versus* time was measured by laser scanning confocal microscopy. The intensity ratios of the two fluorescent dyes were used to determine the internal pH profiles of the membranes in buffer solutions of various pH or glucose levels.

***Results.*** The internal pH was found to be lower than the external pH of buffer solutions. The pH decreased with an increase in glucose concentration, incubation time and the distance towards the center of the membranes due to the relative rates of glucose oxidation and solute diffusion.

***Conclusions.*** The results provided direct experimental evidence of acidic internal pH that inversely related to external glucose concentration in an external medium of constant neutral pH.

**KEY WORDS:** fluorescence ratiometry; glucose-dependent internal pH; internal pH mapping and kinetics; pH-responsive nano-hydrogels; polymeric composite membranes.

## INTRODUCTION

Stimuli-responsive polymers have found broad biomedical and pharmaceutical applications due to their "intelligent" response to environmental triggers such as changes in pH, temperature, ionic strength, glucose concentration, light, and electrical currents (1–21). Of various kinds of polymers, pH-sensitive polymers have been employed in the design of delivery systems for glucose-responsive insulin release (6–16,22). In such systems, glucose oxidase (GOx) is normally incorporated to catalyze glucose oxidation that produces gluconic acid in relation to glucose concentration. It has been postulated that the resultant acid within the delivery systems causes pH reduction, gel swelling (in case of cationic hydrogels) or shrinking (in case of anionic gels), or polymer erosion, leading to faster insulin release at higher glucose levels. Being operated by this mechanism, the effectiveness of the insulin delivery systems *in vivo* is determined by the local pH and pH change rate within the delivery systems as the pH of external medium normally remains constant.

In previous research, we developed polymeric composite membranes that altered their permeability to solutes in response to changes in temperature, pH, and glucose concentration (16–22). These membranes were made from stimulus-responsive nanoparticles of poly(*N*-isopropylacrylamide-co-methacrylic acid) (poly(NIPAAm/MAA)) (23–25) dispersed in an inert polymer matrix. Previous studies showed that the environment-dependent solute permeation through the membranes was in line with but in the opposite direction of the volume change of the nanoparticles (16–21). As the nanoparticles shrank at lower pH, for example, larger pores were generated in the membranes enabling faster solute diffusion, as visualized under an atomic force microscope (21). With immobilized GOx and catalase, the pH-sensitive membranes acquired glucose-responsiveness. Insulin permeability across the membranes increased over 3- to 8-fold when the glucose concentration was raised from 50 to 200 or to 400 mg/dl at 37°C, and returned to the baseline when the glucose concentration was reduced to the original low level (14). We observed that factors influencing pH inside the membranes affected membrane responsiveness noticeably, which include the concentration and activity of the immobilized GOx, the ratio of GOx to catalase (an enzyme to recover partial oxygen consumed by glucose oxidation), and the buffer capacity of the medium. Nevertheless, rational design of the membrane system and prediction of the rate of insulin permeation through the membranes cannot be realized without knowing the pH profiles and kinetics in micro-

[1] Leslie Dan Faculty of Pharmacy, University of Toronto, Toronto, ON M5S 3M2, Canada.
[2] Institute of Biomaterials & Biomedical Engineering, University of Toronto, Toronto, ON M5S 3E1, Canada.
[3] To whom correspondence should be addressed. (e-mail: xywu@phm.utoronto.ca)

domain of the thin membranes (~100 μm) in relation to external glucose levels.

The approach to using pH-responsive polymers and GOx has been found operative in regulating insulin release (6–16), and model simulation has indicated glucose-dependent pH and pH gradients in GOx-containing cationic membranes (26). Nevertheless, up to date few investigations have been carried out to measure the extent and kinetics of pH change *in situ* and in real time within microdomain of a glucose-responsive insulin delivery device during a substrate-enzyme (glucose-GOx) reaction. It is uncertain whether the pH inside a device in particular a thin membrane could remain acidic if the external buffer is kept at pH 7.4; and how fast and to what extent the internal pH would drop in relation to the elevation of glucose concentration. As the indirect glucose-responsive systems rely on the internal pH change to attenuate the membrane permeability (5,6), without knowing the actual internal pH and its kinetics in response to external glucose concentration, the design of self-regulated insulin delivery systems still depends on the experience and trials. To verify the proposed mechanism and to design glucose-responsive insulin delivery systems rationally, it is necessary to measure the temporal and spatial pH distribution inside the membranes on exposure to various pH buffers and glucose concentrations involving a substrate-enzyme reaction.

In early attempts, pH indicators and UV spectrophotomer or fluorometers were employed to determine the internal pH in polymeric membranes (8). However, this approach is limited, as spectrophotometry or fluorometer can not provide the capacity needed for internal spatial pH mapping and kinetic study of the glucose-responsive or pH-sensitive membranes *in situ*. The combination of pH-sensitive fluorescent dyes and optical-sectioning capacity of laser scanning confocal microscopy (LSCM), in contrast, offers the advantages of excellent labeling efficiency, high-resolution spatial mapping, and quantitative and noninvasive measurement of pH inside a microsystem (21,27–36). This approach also allows for the measurement of pH change in microdomains *in situ* in real time. Recently, fluorescent dye ratiometry and LSCM were used to quantitatively investigate the internal pH and pH kinetics of biodegradable poly(lactide-co-glycolide) microspheres (30), plant tissues (33,34), and pharmaceutical pellets and hydrogel structural changes (35,36). In these studies, two fluorescent dyes were physically incorporated in the microsystem at a certain ratio, one as the pH indicator and the other, relatively pH-insensitive, used as the internal reference. This method was reported to eliminate uneven spatial fluorescent dye distribution and photobleaching problems in dynamic internal pH measurement for polymer microspheres and cells (30,33,34). This approach was previously used to monitor internal pH change of poly(lactide-co-glycolide) microspheres due to biodegradation (30). The data were collected at intervals of 1 day or longer. For the application of GOx-responsive insulin delivery, however, fast pH change in a short time, e.g. a few minutes, is desirable, which adds a new challenge to the experiment. Besides, under a condition of clinical application, the internal pH in the GOx-responsive delivery system is expected to span from nearly neutral to weak acidic due to the buffer effect of body fluid. Apparently previously used fluorescent dyes that are effective at pH below 3.5 are not applicable to the insulin delivery system. Hence new suitable fluorescent dyes need to be identified.

The present study was designed to verify the operative mechanism of the pH- and glucose-responsiveness of the membranes and its factors by direct measurement of the kinetics and distribution of pH in the microdomain inside the polymeric composite membranes in response to external pH and glucose concentration. The finding of this study may facilitate rational design and optimization of the membrane system for glucose-responsive insulin delivery. To avoid potential problems of fluorophore changes during the measurement and non-uniform immobilization of the dye, and to overcome other barriers mentioned above, two fluorescent dyes were mixed simultaneously with the pH-sensitive nano-hydrogels, and then incorporated into the membrane. LSCM was employed to measure the fluorescence intensity of the two dyes in thin membranes ~100 μm in thickness at various spatial and temporal points, which, together with ratiometry, provided information of internal pH gradient and kinetics in the membranes.

## EXPERIMENTAL

### Materials

*N*-isopropylacrylamide (NIPAAm, Eastman Kodak) was purified by recrystallization in hexane and toluene. Methacrylic acid (MAA, Sigma-Aldrich) was made inhibitor free by distillation. *N*,*N*′-Methylene-bis-acrylamide (BIS), potassium persulfate (KPS), fluorescein isothiocyanate-dextran (FITC, $M_w$, 4,000), glucose oxidase (type X-S, from *Aspergillus niger*, 50,000 unit), and catalase (*Aspergillus niger*) were purchased from Sigma. Sodium dodecyl sulphate (SDS) and dextrose (anhydrous D-glucose) were from Fisher Scientific. Dibutyl sebacate was a gift from Morflex Inc. Ethylcellulose (viscosity 45, Dow chemical), Texas red-dextran (T-Red, $M_w$, 3,000, Molecular Probes) and other chemicals were used as received unless otherwise specified.

### Synthesis of Poly(NIPAAm/MAA) Nanoparticles

Poly(NIPAAm/MAA) nanoparticles were synthesized by an aqueous dispersion polymerization process (23,37). NIPAAm, MAA and BIS, at a mole ratio of 1:1:0.136, were dissolved in distilled deionized (DDI) water to give a total concentration of 135 mM. SDS (0.4 mM) was used to stabilize the nanoparticles produced. After purging the reaction mixture with $N_2$, potassium persulfate (2.1 mM) was added to initiate the polymerization. The polymerization was carried out at 70°C under the $N_2$ blanket for 4 h with stirring at 200 rpm. The nanoparticles were purified by membrane dialysis using dialysis tubing (Molecular weight cutoff: 12,000 to 14,000, Fisher Scientific) in DDI water. The average diameter of the nanoparticles was determined to be about 500 nm at pH 7.4 by a dynamic laser scanning particle sizer (NICOM 380).

### Preparation of Fluorescence-Labeled Composite Membranes

The membranes were prepared using a method described before (16–22) with modification. In a typical preparation, 0.16 g of poly(NIPAAm/MAA) nanoparticles

were mixed gently with a magnetic stirrer with 16 μg of FITC and 8 μg of T-Red in 3 ml of absolute alcohol at about 4°C in a dark place overnight. The fluorescence-labeled nanoparticles were then mixed with 7 ml of alcohol solution containing 0.24 g of ethylcellulose under the same condition until a homogeneous mixture was obtained. The mixture was poured into dishes to cast membranes with a thickness of ~100 μm after evaporation of the solvent. The membranes were then rinsed with PBS 7.4 to remove unincorporated fluorescent dyes. The resultant pH-sensitive membranes contained 35% (*w*/*w*) nanoparticles. The quantity of FITC and T-Red remained in the membrane was determined to be about 11–12 μg and 5–6 μg respectively.

The glucose-responsive membrane was prepared following the procedure reported in a previous study (16). In a typical preparation, to distribute the enzymes and nanoparticles homogeneously in the membrane, a two-step process was employed. In the first step, 5 mg of glucose oxidase and 1.44 mg of catalase were dissolved in 80 μl of deionized distilled water to prepare an enzyme solution. The enzyme solution was added into the fluorescent dye-entrapped nanoparticles alcohol solution and stirred gently for 8 h at 4°C in a dark place until a homogeneous status was achieved. In the second step, the nanoparticle-enzyme mixtures were mixed with 7 ml of alcohol solution containing 0.24 g of ethylcellulose and various amounts of dibutyl sebacate, a plasticizer. The mixture was stirred gently for overnight at 4°C in a dark place. The mixture was finally used to cast the membrane consisting of 40% (*w*/*w*) nanoparticles and 5% (*w*/*w*) plasticizer.

### Determination of Internal pH

The internal pH of the membranes was determined by the ratiometric imaging method based on the intensity ratio of FITC and T-Red. All the membranes were incubated in PBS 7.4 for overnight to reach equilibrium before exposure to PBS of various pHs or glucose PBS solution. An Olympus Fluoview 300 laser scanning confocal microscope (LSCM; Olympus, Japan) equipped with blue Argon light source (488 nm) and a green HeNe light source (543 nm) was employed to measure the intensities of the dyes at ambient temperature. To minimize cross-talking between FITC and T-Red, FITC was excited at 488 nm and its emission was collected by using a 510/530 nm band-pass filter. T-Red, as an internal reference for the measurement of pH inside the membranes, was sequentially excited at 543 nm and collected by using a 610 nm high-pass filter. The structure of the membranes and the principle of the determination are illustrated in Fig. 1.

For the measurement of pH inside membranes without the enzymes, a membrane sample was mounted in an Attofluor imaging chamber and incubated with 3 ml of phosphate buffer solution (PBS) with varying pH and an ionic strength of 0.15 M for over 20 min at room temperature before scanning. The adequacy of incubation duration for equilibration of the membranes was confirmed by a kinetics study in which fluorescence signals were monitored continuously up to 60 min. No intensity change after 20 min of incubation was observed.

For the study of glucose-responsive pH profile and kinetics inside the membranes, glucose solutions in two different buffer systems were used: (1) pH 7.4 saline solution,

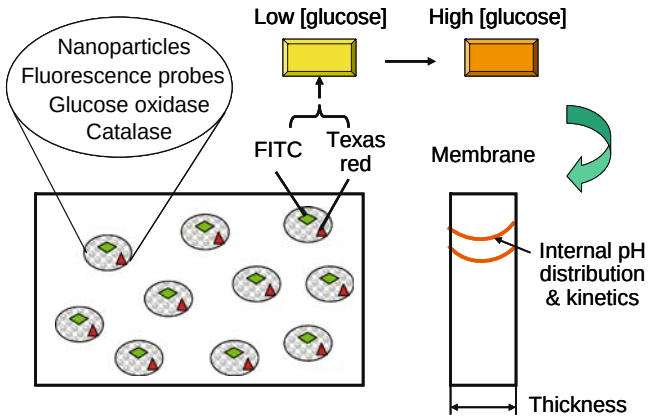


**Fig. 1.** Schematic illustration of the structure of a FITC/T-Red-labeled glucose-responsive polymeric composite membrane and the principle for internal pH mapping in this study.

where the pH of 0.15 M NaCl solution was adjusted to pH 7.4 by addition of 0.01 N NaOH, and (2) pH 7.4 PBS (0.15 M) that comprised 10 mM PBS and 0.14 M NaCl. Initially, an enzyme-containing membrane sample was immersed in 50 mg/dl glucose solution in pH 7.4 saline to investigate internal and external pH change with time. For studies under a constant external pH condition, the membranes were first immersed in pH 7.4 PBS (0.15 M) to saturate the membrane. Then 0.5 ml of concentrate glucose buffer solution at pH 7.4 was added to the chamber to adjust the glucose concentration to 100, 150, 200, and 400 mg/dl respectively. LSCM images were taken at 0, 5, 10, 20 and 40 min after the addition of glucose solution. The pH inside the membrane during the reaction was calculated based on the standard curve obtained from solutions of the dyes (see the description below), while the pH in the medium was measured with a pH meter.

The fluorescence images were acquired under the following settings. A ×10 objective with a numerical aperture of 0.3 was in place to obtain a field of view including both the membrane and surrounding buffer solution. Imaging parameters such as photomultiplier (PMT), gains, laser power, and confocal apertures were tuned to avoid the saturation of each individual fluorescent channel. Fluorescent emissions for FITC and T-Red of the membrane were sampled by acquiring a 512× 512 pixel image for each dye every 2.75 μm step in the Z-direction up to ~50 μm, i.e., the half-thickness of the membranes. The ratio of FITC and T-Red intensity inside the membrane was analyzed using image analysis package (ImageJ) and plugins available at NIH website (http://rsb.info.nih.gov/ij/).

### Determination of Standard Curve

FITC and T-Red at a ratio of 2:1 (*w*/*w*) were dissolved in 0.15 M PBS of various pH. The solutions were introduced to an Attofluor imaging chamber and scanned with LSCM at the excitation and emission wavelengths for FITC and T-Red respectively as presented above. Each experiment was run in triplicate and the average and the standard deviation were reported. LSCM scanning of PBS was carried out to confirm that the autofluorescence from the buffer solutions was negligible and to detect the leakage of fluorescent dyes into

the solution during the experimental process. A standard curve was prepared based on the emission intensity ratio of FITC to T-Red *versus* pH.

## RESULTS

### Fluorescence Intensity and Intensity Ratio of FITC and T-Red *versus* pH

Structurally, the pH-sensitivity of fluorescent dyes is due to a reconfiguration of the fluorophore's π-electron system that occurs upon protonation. Fluorescent dyes like FITC with ionizable substitutes provide pH-sensitivity. The pH sensitivity of FITC and pH insensitivity of T-red was caused by their different chemical structures. Figure 2a presents the fluorescence intensity of FITC and T-Red at a ratio of 2:1(*w*/*w*) in PBS as a function of pH ranging from 4.0 to 7.4. The fluorescent intensity of FITC increases significantly with increasing pH, while the intensity of T-Red maintains steady. This result is consistent with the observation reported by other groups (31,32) and confirms that T-Red is a good candidate for an internal reference.

Figure 2b shows a linear relationship between the intensity ratio of FITC/T-Red and pH within the pH range from 5.0 to 7.4 in PBS. The good correlation between the intensity ratio and pH rationalizes the use of fluorescence ratiometry for the measurement of pH inside the membranes. The linear correlation function, $Intensity\ ratio = 5.942 \times pH - 28.23$ , was used as a standard curve for the calculation of internal pH from 5.0 to 7.4. The intensity ratio of FITC/T-Red was determined to be 1, 7.9, 13, and 15 when the pH of the PBS was 5, 6, 6.8, and 7.4 respectively. For the pH lower than 5.0, the second correlation was used.

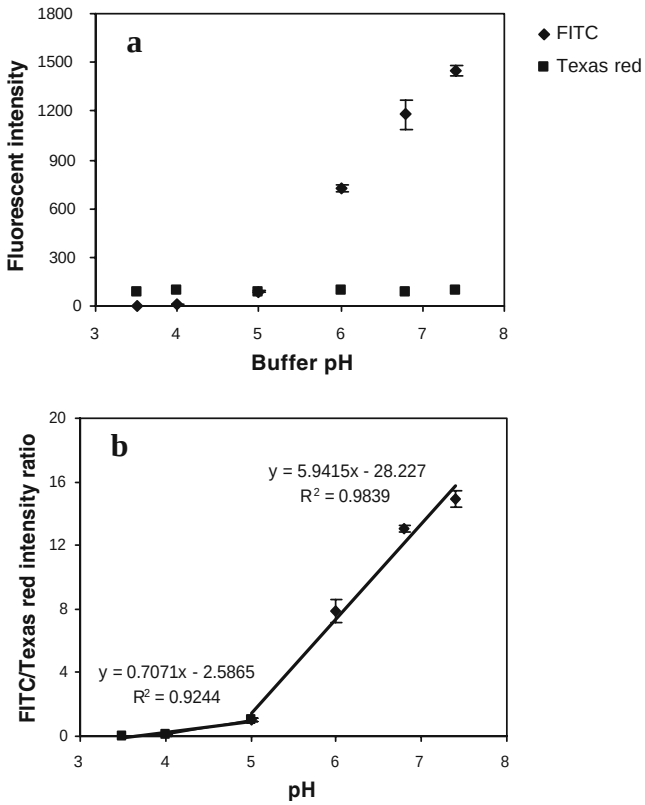


**Fig. 2.** The dependence of **a** fluorescence intensity of FITC and T-Red and **b** their intensity ratio on buffer pH ranging from 3.5–7.4 ($n$= 3). The weight ratio of FITC to T-Red in the buffer solution was 2:1.

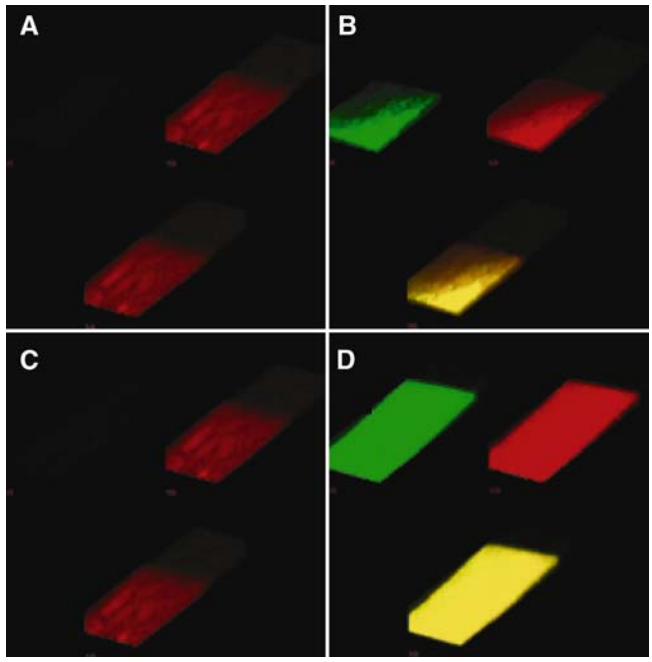


**Fig. 3.** Three-dimensional LSCM images of a pH-sensitive membrane without (**A**) and with FITC and T-Red at a ratio of 2:1 (*w*/*w*) (**B**), and images of glucose-responsive membrane without (**C**) and with the dyes (**D**). The green slab on the top left of each figure stands for the fluorescent intensity at Ex 488 nm/Em 520 nm. The red slab on the top right stands for the fluorescence intensity at Ex 543 nm/Em 610 nm. The slab at the bottom stands for the superimposition of the two images on the top. Slabs on the *top left* in Fig. 4**A** and **C** were unable to be constructed because the fluorescent intensity at Ex 488 nm/Em 520 nm was too weak to be detected.

### LSCM Images of Control Membranes and Fluorescence-Labeled Membranes

LSCM imaging of control membranes (i.e., the membranes without fluorescent dyes) was performed to check whether there were artifacts caused by the autofluorescence of the membranes. Figure 3 presents the three-dimensional LSCM images of a pH-sensitive membrane without (A) and with the dyes (B), and a glucose sensitive membrane without (C) and with the dyes (D). The images were acquired at 488 nm/Em 520 nm (the green slabs on the top left) and at Ex 543 nm/Em 610 nm (the red slabs on the top right), the same wavelengths as those employed for measuring intensities of FITC and T-Red respectively. The slabs at the bottom are superimposition of the two images on the top. Note that the green slabs are invisible in Fig. 3A and C for the control membranes as the intensity was too weak to be detected.

This result suggests that autofluorescence of the control membranes would not affect the intensity values of FITC distributed in the membranes. The intensity of the control membranes at Ex 543 nm/Em 610 nm is very weak with ca. 11 as compared to over 130 for the same membranes containing T-Red. Despite this, the intensity of autofluoresence of the

membranes at Ex 543 nm/Em 610 nm was deducted from the intensity of T-Red in the calculation of internal pH. Figures 3B and 3D show strong fluorescent signals of FITC and T-Red detected from both fluoresecnece-labeled membranes. They also evidence homogeneous distribution of the fluorescent dyes, demonstrating the effectiveness of the labeling protocol used in this study.

Figure 4A to E are typical LSCM images of FTIC/T-Red labeled glucose-responsive membranes that were incubated in 400 mg/dl glucose PBS for various times. The internal pH of the membranes at (A) 0, (B) 5, (C) 10, (D) 20, and (E) 40 min was determined to be 6.2, 5.4, 5.3, 5.2 and 5.1 respectively. The time-course images suggest that the fluorescence of FITC and T-Red was retained during the whole reaction process. This prolonged fluorescence signals may be credited to the presence of catalase, without which the membranes showed diminishing fluorescence signals with time as seen in the preliminary tests (data not shown). The effect of catalase on the stability of signals may be explained as follows. The strong oxidizer, hydrogen peroxide produced by glucose oxidation, may degrade FITC and T-Red causing the loss of the fluorescent signals. The use of catalase to convert hydrogen peroxide to oxygen and water helps maintain the fluorescence signals of the dyes, in addition to preserving the bioactivity of GOx as observed in our previous work (16).

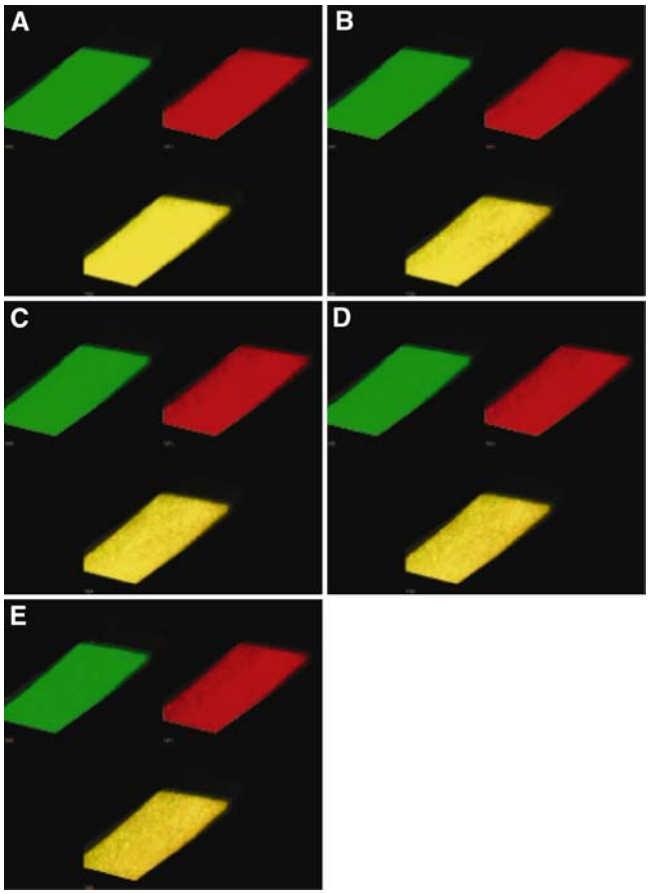


**Fig. 4.** LSCM images of a FITC/T-Red labeled glucose-responsive membrane incubated in 400 mg/dl glucose PBS (ionic strength: 0.15 M) at **A** 0 min; **B** 5 min; **C** 10 min; **D** 20 min; and **E** 40 min.

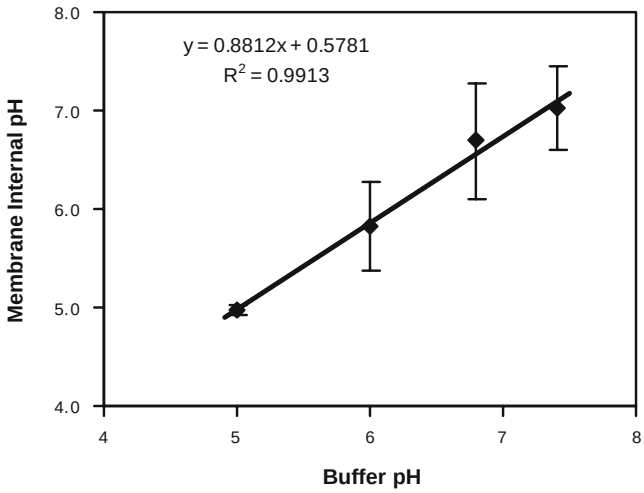


**Fig. 5.** Internal pH of a FITC/T-Red-labeled pH-sensitive membrane with 35% nanoparticles *versus* buffer pH. The membrane was incubated in 0.15 M PBS of various pH ($n$=3).

## Internal pH of pH-Sensitive Membranes

Figure 5 depicts that the internal pH of a membrane without the enzymes is lower than the buffer pH at pH above 5.0. As the buffer pH increases from 5.0 to 7.4, the internal pH raises from 5.0 to 7.0 linearly. At buffer pH 4.0, the fluorescence intensity of FITC was close to the detection limit. Hence the determined internal pH is not reported here due to a concern about its reliability.

## Kinetics of pH inside the Glucose-Responsive Membranes

Figure 6 illustrates the internal and external pH *versus* time for a glucose-responsive membrane immersed in 50 mg/dl glucose saline solution for one hour. Note that the internal pH at a given time is an average of 23 pH values measured along the half thickness of the membrane. The internal pH of the membrane drops from 6.0 to 4.9 in the first 10 min and

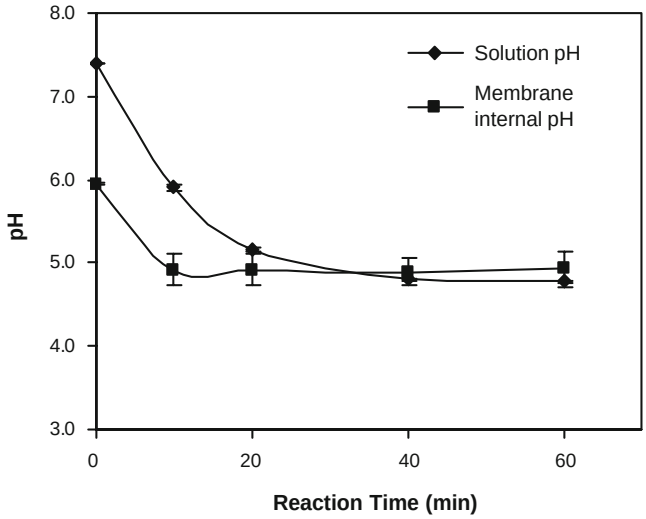


**Fig. 6.** Internal and external pH kinetics of a glucose-responsive membrane in response to 50 mg/dl glucose saline solution ($n$=3).

then maintains at this value for the rest of the time. The pH of the medium decreases rapidly from 7.4 to 5.9 within 10 min, and gradually decreases to about 4.8. In the beginning the internal pH is lower than the external one, and then becomes almost the same as that of the medium. This result evidences the bioactivity of glucose oxidase immobilized in the membrane, in agreement with our previous observation (16), which lowers internal pH in the presence of glucose.

Since under the *in vivo* condition, the physiological fluid has a strong buffer capacity and is continuously refreshed, we measured the internal pH in 0.15 M pH 7.4 PBS with varying glucose levels. Figure 7 portrays the internal average pH profiles of glucose-responsive membranes in 100, 150, 200, and 400 mg/dl glucose in this buffer for up to 40 min. It can be seen that the internal pH decreases dramatically in the first 5 to 10 min, and the higher the glucose concentration, the faster the change. After 10 min, the curves approach plateaus with the lower internal pH corresponding to higher glucose levels. The internal pH is 5.8, 5.5, 5.3 and 5.1 respectively for the membranes in 100, 150, 200, and 400 mg/ml glucose PBS solutions. This finding is very important as it has provided direct evidence to support the mechanism that the glucose-dependent permeation of the composite membrane is due to the pH reduction within microdomain of the membrane. The short response time of 5–10 min is also in line with our previous observation that the increment in insulin release occurred in 5 min upon a step increase in glucose concentration (16).

### pH Gradient inside the Glucose-Responsive Membranes

The optical-sectioning capacity of LSCM was utilized to study spatial pH distribution inside the glucose-responsive membranes. Owing to the symmetry of the membrane geometry, only a half of the membrane thickness was scanned. Figure 8 portrays the pH profiles of the membranes in buffer solutions of various glucose concentrations at 40 min. Obviously pH gradients exist in all samples with the lowest pH in the center of the membranes. The central pH differs from the peripheral pH by a 0.2 to 0.3 pH unit. This difference tends to increase with increasing glucose concentration. Besides, the internal pH is consistently lower for membranes in solutions of higher glucose concentrations, as we hypothesized and is in agreement with previous model prediction (26).

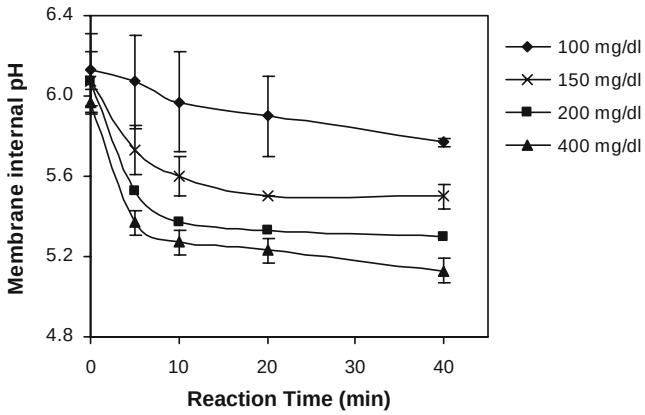


**Fig. 7.** Internal pH kinetics of glucose-responsive membranes in 100, 150, 200, and 400 mg/dl glucose pH 7.4 PBS at room temperature ($n$= 3). The pH of the external medium remained at 7.4 during the entire period.

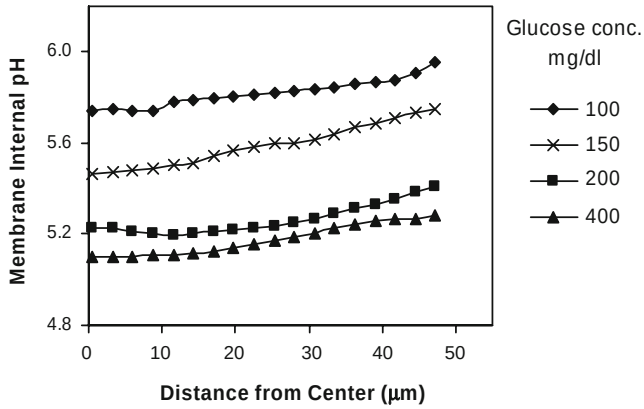


**Fig. 8.** Typical pH profiles within glucose-responsive membranes along the distance from the center to the edge of the membranes immersed in 100, 150, 200, and 400 mg/dl glucose PBS respectively for 40 min.

One may be concerned about a possible error in the results presented above, introduced by the leakage of fluorescent dyes from the membranes during the test. Nevertheless, no leakage of fluorescent dye was detected in the external media. Even if there were minor leakage affecting the absolute intensities of the fluorescent dyes, the intensity ratio of the two dyes would not be affected as long as their ratio remains constant during experiments. This is one of the advantages of the ratiometric method.

## DISCUSSION

The lower internal pH of the pH-sensitive membranes shown in Figure 5 may be ascribed to the acidic polyelectrolyte nature of the nanoparticles. These nanoparticles are made of cross-linked poly(NIPAAm/MAA), essentially a weak polyacid with a p$K$a about 5.5 (22). Its ionization degree increases with pH as predicted from the extended Henderson–Hasselbalch equation (5)

$$\mathrm{pH} = \mathrm{p}K_a\, n_0 \log\alpha/(1-\alpha) \tag{1}$$

where $n_0$ is the fraction of ionizable groups in the polymer and $\alpha$ denotes the ionization degree of these groups. As pH is increased from 4.0 to 7.4, the ionization degree of poly (NIPAAm/MAA) nanoparticles increases from 0.09 to over 0.99 (22). In other words, their polyelectrolyte nature is augmented by increasing pH.

According to the theory of Donnan equilibrium, the concentration of hydrogen ions inside a swollen polyelectrolyte gel in equilibration with a buffer solution is correlated with the concentration in the medium by the following equation (26,38):

$$C_{\mathrm{H}^+} = \lambda^z C'_{\mathrm{H}^+} \tag{2}$$

where $\lambda$ is the Donnan ratio, $z$ is the valance of the ions in the buffer, and $C_{\mathrm{H}^+}$ and $C'_{\mathrm{H}^+}$ are respectively the ionic

concentration in the gel and in the external solution. With a rather complex computational procedure (26), we can demonstrate that λ is greater than unity for anionic polymers and thus $C_{H^+}$ is higher than $C'_{H^+}$. In other words, the internal pH is lower than the external pH as predicted by the theory.

Unlike in the experiment using saline solution where internal and external pH kinetic curves merged after 40 min (Fig. 6), the 0.15 M PBS remained at 7.4 at all glucose levels during the entire testing period, regardless the variation in the equilibrium internal pH with glucose concentration. This result directly supports our hypothesis that the microenvironmental pH inside glucose-responsive membranes was lower than the medium pH and agrees with other group's report that the pH of the microenvironment of the immobilized enzyme was lower than that in the bulk buffer solution (39). Since the internal pH of the membranes was in a narrow range (i.e., pH 5–6) in this study, the bioactivity of glucose oxidase in response to varying glucose concentration should remain steady, which differs from the observation made by others in a much lower pH range (39).

The glucose concentration-dependent pH, pH gradient, and pH kinetics inside the enzyme-containing membranes is controlled by a dynamic process of reaction and diffusion of involved species. As illustrated in Fig. 9, glucose diffuses from the external medium into the membrane and is then oxidized by the immobilized GOx. This reaction generates gluconic acid inside the membrane, which then diffuses out of the membrane owing to a concentration gradient. When the rate of glucose oxidation is greater than the diffusion rate of gluconic acid, the acid is accumulated in the membrane leading to pH reduction. As the diffusion distance is longer for the acid closer to the center of the membrane, the accumulation of the acid is more marked.

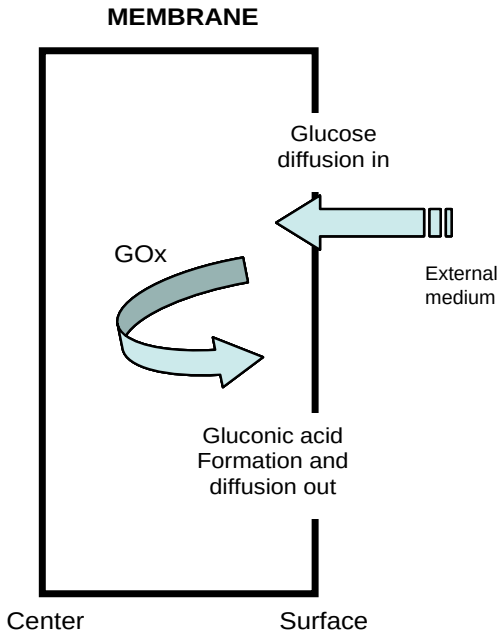


**Fig. 9.** Schematic illustration of a dynamic process of diffusion and reaction of involved species for a glucose-responsive membrane in a glucose buffer solution.

Although the membrane was initially saturated with pH 7.4 PBS, the quantity and buffer capacity of the PBS are not enough to maintain the pH inside the membrane. Consequently the internal pH is much lowered by the accumulation of the acid. Even if the external pH remained at pH 7.4, the pH inside the membrane decreases with increasing glucose concentration owing to the relatively higher rate of glucose diffusion and oxidation at higher glucose concentration than those at lower glucose concentrations. This relative rate of reaction and diffusion imparts the glucose-responsive pH change to the membranes.

As shown in Fig. 6, the pH kinetic profiles inside and outside the membrane show a similar trend but the latter shows a slower pace. This phenomenon can also be explained by the relative rates of glucose oxidation and gluconic acid diffusion at different stages. In the beginning, gluconic acid is quickly produced by glucose oxidation which accumulates in the membrane causing internal pH drop due to faster reaction than diffusion. Later as more and more gluconic acid diffuses out to the medium due to a concentration gradient, a decrease in the external pH occurs because of inadequate buffer solution (3 ml) and buffer capacity of the medium. That the pH reaches a plateau after 20 min is attributable to the exhaustion of glucose in the medium, while the merge of the internal and the external pH curves implies that a diffusion equilibrium is established in a finite liquid volume (40).

Both Figs. 7 and 8 show that internal pH of the membrane does not change significantly when the glucose concentration increases from 200 to 400 mg/dl. This result may be caused by the limited supply of oxygen for the glucose oxidization. Our previous model simulation demonstrated that when the rate of glucose oxidation is high, e.g. in the case of either a high glucose level or a high GOx loading, the reaction becomes oxygen-limited (26). Further investigation is needed to improve the supply of oxygen by changing formulation if it is a concern.

## CONCLUSIONS

This work has demonstrated the utility of fluorescence ratiometry and LSCM in the characterization of temporal and spatial pH profiles in a substrate-enzyme reaction process within a thin membrane. The pH distribution and pH kinetics of the microdomains inside the pH- or glucose-responsive polymeric composite membranes have been successfully determined by LSCM using the intensity ratio of FITC and T-Red. This work has provided, for the first time, direct evidence of glucose-responsive pH gradient and kinetics in the composite membranes, and lower internal pH than the external pH in a thin pH-sensitive membrane. It has been found that the magnitude and the speed of pH reduction and the pH gradient inside the membranes increase with increasing glucose concentration even in a buffer of constant pH. These results have verified the previously proposed mechanism that glucose oxidation induced internal pH reduction is a key factor that triggers shrinkage of the pH-sensitive poly(NIPAAm/MAA) nanoparticles thus regulating insulin release through the composite membranes. The direct visualization of internal pH distribution and kinetics has useful utilization in the rational design of such kind of glucose-responsive membranes for self-regulated insulin delivery with desired rates.

## ACKNOWLEDGMENT

This research is sponsored by the Natural Sciences and Engineering Research Council of Canada. The University of Toronto Open Fellowship and Ben Cohen Fund provided to H.Y. Huang are also gratefully acknowledged.

## REFERENCES

1. J. Kost and R. Langer. Responsive polymeric delivery systems. *Adv. Drug Deliv. Rev.* **46**:125–148 (2001).
2. Y. Qiu and K. Park. Environment-sensitive hydrogels for drug delivery. *Adv. Drug Deliv. Rev.* **53**:321–339 (2001).
3. T. Miyata, T. Uragami, and K. Nakamae. Biomolecule-sensitive hydrogels. *Adv. Drug Deliv. Rev.* **54**:79–98 (2002).
4. A. Chi and T. Okano. Pulsatile drug release control using hydrogels. *Adv. Drug Deliv. Rev* **54**:53–77 (2002).
5. X. Y. Wu, Q. Zhang, and R. Arshady. Stimuli sensitive hydrogels. Polymer structure and phase transition. In R. Arshady (ed.), *Polymeric biomaterials*, Citus Books, London, UK, 2003, pp. 157–194.
6. X. Y. Wu, Q. Zhang, and R. Arshady. Stimuli sensitive hydrogels. Response and release modulation. In R. Arshady (ed.), *Polymeric biomaterials*, Citus Books, London, UK, 2003, pp. 195–231.
7. T. Traitel, Y. Cohen, and J. Kost. Characterization of glucose-sensitive insulin release systems in simulated *in vivo* conditions. *Biomaterials* **21**:1679–1687 (2000).
8. W. G. Albin, A. T. Horbett, R. S. Miller, and L. N. Ricker. Theoretical and experimental studies of glucose sensitive membranes. *J. Control. Release* **6**:267–291 (1987).
9. K. Ishihara and K. J. Matsui. Glucose-responsive insulin release from polymer capsule. *Polym. Sci. Polym. Lett. Ed.* **24**:413–417 (1986).
10. R. A. Siegel and B. A. Firestone. Mechanochemical approaches to self-regulating insulin pump design. *J. Control. Release* **11**:181–192 (1990).
11. K. Podual, F. J. Doyle III, and N. A. Peppas. Glucoes-sensitivity of glucose oxidase-containing cationic copolymer hydrogels having poly(ethylene glycol) grafts. *J. Control. Release* **67**:9–17 (2000).
12. Y. Ito, M. Casolaro, K. Kano, and T. Imanishi. An insulin-releasing system that is responsive to glucose. *J. Control. Release* **10**:195–203 (1989).
13. E. Kokufuta, S. Matsukawa, T. Ebihara, and K. Matsuda. Construction of biochemo-mechanical systems using polyelectrolyte gels. In K. S. Schmitz (ed.), *Macro-ion characterization, from dilute solutions to complex fluids, ACS Symp. Series 548*, ACS, Washington, DC, 1994, pp. 507–516.
14. J. Heller, A. C. Chang, G. Rodd, and G. M. Grodsky. Release of insulin from pH-sensitive poly(ortho esters). *J. Control. Release* **13**:295–302 (1990).
15. L. Ying, E. T. Kang, and K. G. Neoh. Covalent immobilization of glucose oxidase on microporous membranes prepared from poly (vinylidene fluoride) with grafted poly(acrylic acid) side chains. *J. Memb. Sic.* **208**:361–374 (2002).
16. K. Zhang and X. Y. Wu. Modulated insulin permeation across a glucose-sensitive polymeric composite membrane. *J. Control. Release* **80**:169–178 (2000).
17. F. Yam and X. Y. Wu. A novel composite membrane for temperature responsive permeation. *Polymer Preprint* **40**:312–313 (1999).
18. F. Yam, X. Y. Wu, and Q. Zhang. A novel composite membrane for temperature and pH responsive permeation. In K. Park (ed.), *Controlled drug delivery: designing technology for the future*, ACS, Washington, DC, 2000, pp. 263–272.
19. X. Y. Wu and F. Yam. Polymer System for Drug Delivery and Solute Separation, US patent, 2003, US 6,565,872.
20. K. Zhang and X. Y. Wu. Temperature- and pH-responsive polymeric composite membranes for regulated delivery of peptide and protein drugs. *Biomaterials* **25**:5281–5291 (2004).
21. K. Zhang, H. Y. Huang, G. C. Yang, J. Shaw, C. Yip, and X. Y. Wu. Characterization of nanostructure of stimuli-responsive polymeric composite membranes. *Biomacromolecules* **5**:1248–1255 (2004).
22. K. Zhang, C. Quan, H. Huang, N. Taulier, and X. Y. Wu. On the stability of insulin delivered by a new glucose-responsive polymeric composite membrane. *J. Pharm. Pharmacol.* **56**:611–620 (2004).
23. X. Y. Wu and P. I. Lee. Preparation and characterization of thermal- and pH-sensitive nanospheres. *Pharm. Res.* **10**:1544–1547 (1993).
24. J. Huang and X. Y. Wu. Effect of pH, salt, surfactant and composition on phase transition of poly(NIPAm/MAA) nanoparticles. *J. Poly. Sci: Poly. Chem.* **37**:2667–2676 (1999).
25. J. Moselhy, X. Y. Wu, R. Nicholov, and K. Kodaria. *In vitro* characterization of interaction of poly(NIPAm/MAA) nanoparticles with proteins and cells. *J. Biomater. Sci. Polymer Edn.* **11**(2):123–147 (2000).
26. M. Abdekhodaie and X. Y. Wu. Modeling of a glucose-sensitive cationic membrane. *J. Memb. Sci.* **254**:119–127 (2005).
27. R. P. Haugland. Molecular probes handbook of fluorescent probes and research products. 9th edition. Molecular Probes, Eugene, Oregon, 2002.
28. J. Zhang, R. E. Campbell, A. Y. Ting, and R. Y. Tsien. Creating new fluorescent probes for cell biology. *Nat. Rev. Mol. Cell Biol.* **3**:906–918 (2002).
29. M. D. Burke, J. O. Park, M. Srinivasarao, and S. A. Khan. Diffusion of macromolecules in polymer solutions and gels: A laser scanning confocal microscopy study. *Mcromolecules* **33**:7500–7507 (2000).
30. K. Fu, D. W. Pack, A. M. Klibanov, and R. Langer. Visual evidence of acidic environment within degrading poly(lactic-co-glycolic acid) (PLGA) microspheres. *Pharm. Res.* **17**:100–106 (2000).
31. Y. Hirokawa, H. Jinnai, Y. Nishikawa, T. Okamoto, and T. Hashimoto. Direct observation of internal structures in poly (*N*-isopropylacrylamide) chemical gels. *Macromolecules* **32**:7093–7099 (1999).
32. A. Shenderova, T. G. Burke, and S. P. Shwendeman. The acidic microclimate in poly(lactic-co-glycolic) microspheres stabilizes camptothecins. *Pharm. Res.* **16**:241–248 (1999).
33. D. P. Taylor, J. Slattery, and A. C. Leopold. Apoplastic pH in corn root gravitropsim: a laser scanning confocal microscopy measurement. *Physiol. Plant* **97**:35–38 (1996).
34. Q. Yu, J. Kuo, and C. Tang. Using confocal laser scanning microscopy to measure apoplastic pH change in roots of Lupinus angustifolius L. in response to high pH. *Ann. Bot.* **87**:47–52 (2001).
35. S. Cope, S. Hibberd, J. Whetstone, R. MacRae, and C. Melia. Measurement and mapping of pH in hydrating pharmaceutical pellets using confocal laser scanning microscopy. *Pharm. Res.* **19**:1554–1563 (2002).
36. E. Kuwana, F. Liang, and E. Sevick-Muraca. Fluorescence lifetime spectroscopy of a pH-sensitive dye encapsulated in hydrogel beads. *Biotechnol. Prog.* **20**:1561–1566 (2004).
37. X. Y. Wu, R. H. Pelton, A. E. Hamielec, D. R. Woods, and W. McPhee. The kinetics of poly(N-isopropylacrylamide) microgel latex formation. *Colloid Polym. Sci.* **272**:467–477 (1994).
38. R. A. Siegel. Hydrophobic weak polyelectrolyte gels: Studies of swelling equilibria and kinetics. *Adv. Poly. Sci.* **109**:233 (1993).
39. H. W. Blanch, and D. S. Clark. *Biochemical Engineering*. Marcel Dekker, New York, NY, 1996, p. 118.
40. Y. Zhou and X. Y. Wu. Finite element analysis of diffusional drug release from complex matrix systems, I. Complex geometries and composite structures. *J. Control. Release* **49**:277–288 (1997).